Update of LoKI-B simulation tool with electron density growth by electron-impact ionizations

Duarte Gonçalves
Instituto Superior Técnico, Universidade de Lisboa, Lisboa, Portugal
(Dated: September 2017)

New applications for low-temperature plasmas create a technological need to improve the predictability on their behaviour. This work contributes to the development of LoKI-B, an EBE solver, by updating its treatment of electron-impact ionizations, including two-electron density growth models (a spatial and a temporal), and a non-conservative ionization collisional operator that uses a differential ionization cross section. Predictions, for high values of E/N, of the first Townsend ionization coefficient improved in Argon and Nitrogen. Benchmark tests were done against another EBE solver code. An analysis of commonly used ionization collisional operators, questions the use of the equal energy sharing mode.

INTRODUCTION

Since the last century, low-temperature plasmas have been extensively used on the industry of processing materials, with developments in environmental and biological applications being made in recent years. As a result, there is a newfound technological need to improve predictions of low-temperature plasma (LTP) behaviour.

This is the aim of the project KInetic Testbed for PLASMa Environmental and Biological Applications (KIT-PLASMEBA). This project intends to develop new LTP modelling tools, such as a state-of-the-art kinetic scheme named LisbOn KInetics (LoKI). This code contains an electron Boltzmann equation (EBE) solver named LoKI-B.

This work contributes to the development of LoKI-B by updating its treatment of electron-impact ionizations. The goal of this work will then be to include two electron density growth models, as well as a non-conservative ionization collisional operator that uses a differential ionization cross section.

THEORETICAL FORMULATION

The electron Boltzmann equation

The main goal of an EBE solver, is to obtain the electron distribution function by solving the EBE. By expanding the total derivative of the distribution function (assuming that the distribution function may have an explicit time dependence, there can be an electron density gradient, and electrons will be under the influence of an electric field) we arrive at an EBE,

$$\frac{\partial \widetilde{F}}{\partial t}+\vec{v}\cdot\nabla_{\vec{r}}\widetilde{F}-\frac{e\,\vec{E}(t)}{m_e}\cdot\nabla_{\vec{v}}\widetilde{F}=I(\widetilde{F})+J(\widetilde{F})+J_I(\widetilde{F})\ . \quad (1)$$

The solution of equation 1 is the electron distribution function $\tilde{F}$. The collisional operator is divided in elastic collisions I, conservative inelastic/superelastic collisions J, and in non-conservative inelastic ionizing collisions J_I.

The particle distribution function

In this work, the electron distribution function, which is normalized to the electron density n_e,

$$\int_0^\infty \tilde{F}(\vec{r},\vec{v},t)d\vec{v}=n_e(\vec{r},t), \quad (2)$$

will be expanded in various approximations.

The first approximation to be applied is the adiabatic approximation, in which we assume that the spatial dependence of the electron density is similar to the spatial dependence of the distribution function. Meaning that,

$$\tilde{F}(\vec{r},\vec{v},t)\approx n_e(\vec{r},t)\,F(\vec{v},t), \quad (3)$$

with F being a probability distribution function on the electron velocity, normalized to one,

$$\int_0^\infty F(\vec{v},t)d\vec{v}=1. \quad (4)$$

Through this work we will also use the electron energy distribution function (EEDF) which is also a probability function that relates to the electron velocity distribution function as,

$$F(v)\,4\pi\,v^2dv=f(u)\,\sqrt{u}\,du, \quad (5)$$

$$\int_0^\infty f(u,t)\sqrt{u}du=1. \quad (6)$$

We will also expand the electron velocity distribution function F on its velocity components using spherical harmonics. We will assume that the anisotropy is along the z axis, such that the expansion goes as,

$$\vec{F}(\vec{v},t)\approx F^0(v,t)+F^1(v,t)\cos\theta=F^0(v,t)+\vec{F^1}(v,t)\cdot\frac{\vec{v}}{v}, \quad (7)$$

in which θ is the polar angle between the velocity $\vec{v}$ and the anisotropy $\vec{F^1}=F^1\vec{e}_z$. This allows us to separate an isotropic part F^0 and an anisotropic part F^1.

The temporal dependence of the function F will be a response to the varying electric field. Assuming that the electric field varies harmonically with a high frequency ω, we can expand the distribution function in a Fourier series,

$$F(\vec{v}, t) = \sum_m F_m e^{i\,m\,\omega\,t} \approx F^0 + F_0^1 P_1 + F_1^1 P_1 e^{i\,\omega\,t}. \tag{8}$$

The term F_1^0 was assumed to be zero, since $\omega \gg \frac{m_e}{M}\nu_c$, with M being the mass of the neutral particles, m_e the electron mass, and ν_c is the frequency of the quantity of momentum transfer.

Electron-impact ionization

Electron-impact ionization is a process in which an electron collides with a neutral particle producing a positive ion and two other electrons. For bookkeeping purposes, it is customary to call the faster of the two electron as scattered and the slower as secondary. The initial electron will also be distinguished from the electrons produced and will be called the primary electron. In terms of energy we have,

$$0 \leq u_{sec} \leq u_{sca} \leq \epsilon - V_I \ , \tag{9}$$

$$\epsilon = V_I + u_{sca} + u_{sec} \ , \tag{10}$$

with ϵ the primary electron energy, u_{sca} the scattered electron energy, u_{sec} the secondary electron energy, and V_I the ionization potential in eV.

In order to describe the electron energy sharing we can use a differential ionization cross section on the secondary electron's energy,

$$\frac{d\sigma_I(\epsilon, V_I)}{du_{sec}} \equiv q^I_{sec}(\epsilon, u_{sec}). \tag{11}$$

which is also referred to as single differential cross section (SDCS). Integrating this cross section on the secondary electron energy we obtain the total ionization cross section σ_I,

$$\sigma_I(\epsilon, V_I) = \int_0^{(\epsilon - V_I)/2} q^I_{sec}(\epsilon, u_{sec}) du_{sec}. \tag{12}$$

One of the most comprehensive measurements of SDCS was done by Opal, Peterson and Beaty for a number of gases [1, 2]. They used a function that had a similar shape to the data, with a gas specific parameter w, and a normalization constant dependent on the primary electrons energy. Introducing this function in 12, they obtained an expression for the differential ionization cross section,

$$q^I_{sec}(\epsilon, u_{sec}) = \frac{\sigma_I(\epsilon)}{w \arctan\frac{\epsilon - V_I}{2w}} \frac{1}{1 + \left(\frac{u_{sec}}{w}\right)^2} \quad . \tag{13}$$

The ionization collisional operator for electron-impact ionization was showed by Holstein [3] to be,

$$\frac{J_I(u)}{\gamma} = \int_{2u+V_I}^{\infty} \epsilon\, q^i_{sec}(\epsilon, u)\, f(\epsilon)\, d\epsilon + \int_{u+V_I}^{2u+V_I} \epsilon\, q^i_{sca}(\epsilon, u) f(\epsilon)\, d\epsilon - u\, \sigma_I(u)\, f(u). \tag{14}$$

Here $\gamma = \frac{m_e N n_e}{4\pi e\sqrt{u}}$ is a common factor to the all EBE terms, in which N is the gas density. The first term accounts for secondary electrons, the second term for scattered electrons, and the third term to primary electrons. This will be the ionization operator implemented in LoKI.

However, there are also other frequently used ionization collisional operator. The conservative ionization collisional operator, in which there is no production of secondary electrons. The non-conservative collisional operator "one electron takes all", in which secondary electrons have zero energy. And the non-conservative ionization collisional operator with equal energy sharing, in which the scattered and the secondary electrons have the same energy.

Two electron density growth models will be applied. The electron density exponential spatial growth model,

$$n_e(\vec{r}, t) \approx n_e(z, t) = n_e(t)\, e^{\alpha\, z}, \tag{15}$$

assumes that electron density grows with a constant spatial frequency α, the first Townsend ionization coefficient. And the electron density exponential temporal growth model,

$$n_e(\vec{r}, t) = n_e(\vec{r})\ e^{<\nu_I>\, t}, \tag{16}$$

assumes that electron density grows with a constant temporal frequency $\langle\nu_I\rangle$, the mean electron-impact ionization frequency.

Two-term electron Boltzmann equation

By applying these expansions on the EBE we can obtain an equation for the isotropic part, the stationary anisotropic part, and the non-stationary anisotropic part. Substituting one in another, we can obtain equations solely dependent on the isotropic part, that is, the EEDF. Thus, there is an equation for each electron density growth model, and type of electric field, direct current (DC) or high frequency (HF).

Temporal electron density growth with DC electric field

$$-u\frac{C_I}{\sqrt{\frac{2eu}{m_e}}}f(u)+\frac{\partial}{\partial u}\left(\frac{u}{3}\frac{E_{0R}^2}{\sigma_{eff}^I(u)}\frac{\partial f(u)}{\partial u}\right)+\frac{I^0(u)}{\gamma}+\frac{J^0(u)}{\gamma}+\frac{J_I(u)}{\gamma}=0 \tag{17}$$

Temporal electron density growth with HF electric field

$$-u\frac{C_I}{\sqrt{\frac{2eu}{m_e}}}f(u)+\frac{\partial}{\partial u}\left(\frac{u}{3}\frac{E_{1R}^2}{2}\frac{\sigma_{eff}^I(u)}{{\sigma_{eff}^I(u)}^2+\omega_R^2/\frac{2eu}{m_e}}\frac{\partial f(u)}{\partial u}\right)+\frac{I^0(u)}{\gamma}+\frac{J^0(u)}{\gamma}+\frac{J_I(u)}{\gamma}=0 \tag{18}$$

Spatial electron density growth with DC electric field

$$\frac{\alpha_R}{3}\left[\frac{u}{\sigma_eff}\left(\alpha_R f(u)+E_{0R}\frac{\partial f(u)}{\partial u}\right)+\frac{\partial}{\partial u}\left(\frac{u\,E_{0R}}{\sigma_{eff}}f(u)\right)\right]+\frac{\partial}{\partial u}\left(\frac{u}{3}\frac{E_{0R}^2}{\sigma_{eff}(u)}\frac{\partial f(u)}{\partial u}\right)+\frac{I^0(u)}{\gamma}+\frac{J^0(u)}{\gamma}+\frac{J_I(u)}{\gamma}=0 \tag{19}$$

Here quantities with the subscript R are reduced quantities, defined by the original quantity divided by the gas density N, for example $E_{0R}=\frac{E_0}{N}$. The quantity σ_{eff}^I is defined as $\sigma_{eff}^I=\sigma_{eff}+\frac{C_I}{\sqrt{\frac{2eu}{m_e}}}$, in which σ_{eff} is the effective cross section, which is used to write an effective anisotropic collisional operator, and $C_I=\langle\nu_I\rangle/N$ the ionization rate coefficient.

Drift-diffusion equations

The drift-diffusion equations can be calculated through the electron transport $\vec{\Gamma}=n_e\vec{v}_{drift}$. Since the EEDF was expanded in Fourier series, the electron flux will also be expanded,

$$\vec{\Gamma}=\vec{\Gamma}_0+\vec{\Gamma}_1\,e^{i\,\omega\,t}. \tag{20}$$

The drift velocity can by calculated with the anisotropic part of the EEDF

$$\vec{v_{drift}}=\frac{1}{3}\sqrt{\frac{2\,e}{m_e}}\int_0^\infty u\;f^1(u)\;du\vec{e}_z. \tag{21}$$

with f_0^1 for DC fields and f_1^1 for HF fields.

For the DC electric field and temporal growth model the drift-diffusion equation is,

$$\Gamma_0=n_e\mu_0E, \tag{22}$$

with,

$$\mu_0=-\frac{1}{3N}\sqrt{\frac{2e}{m_e}}\int_0^\infty u\frac{1}{\sigma_{eff}^I(u)}\frac{\partial f(u)}{\partial u}du. \tag{23}$$

For the DC electric field and spatial growth model the drift-diffusion equation is,

$$\Gamma_0=-D\nabla_r n_e+n_e\mu_0E, \tag{24}$$

with,

$$D=\frac{1}{3N}\sqrt{\frac{2e}{m_e}}\int_0^\infty u\;\frac{1}{\sigma_{eff}(u)}f(u)du, \tag{25}$$

$$\mu_0=-\frac{1}{3N}\sqrt{\frac{2e}{m_e}}\int_0^\infty u\frac{1}{\sigma_{eff}(u)}\frac{\partial f(u)}{\partial u}du. \tag{26}$$

For HF fields, and temporal density growth, the drift-diffusion equation is

$$\Gamma_1=n_e\mu_1E_1, \tag{27}$$

with $\mu_1=\mu_r+i\,\mu_i$,

$$\mu_r=-\frac{1}{3N}\sqrt{\frac{2e}{m_e}}\int_0^\infty u\frac{\sigma_{eff}^I(u)}{{\sigma_{eff}^I(u)}^2+\omega_R^2/\frac{2eu}{m_e}}\frac{\partial}{\partial u}f(u), \tag{28}$$

$$\mu_i=\frac{1}{3N}\sqrt{\frac{2e}{m_e}}\int_0^\infty u\frac{\omega_R\sqrt{\frac{m_e}{2eu}}}{{\sigma_{eff}^I(u)}^2+\omega_R^2/\frac{2eu}{m_e}}\frac{\partial}{\partial u}f(u). \tag{29}$$

COMPUTATIONAL APPROACH

In order to numerical solve the EBE we need to discretize it into an 1-D energy grid. The grid ranges from 0 up to u_{max}. The energy step will be $\Delta u = u_{max}/n$, being n the number of intervals.

Terms linear on the EEDF are discretized by writing them at the middle of the energy grid intervals. Terms that involve the integration of the EEDF are discretized using the mid-point quadrature rule. Terms that involve EEDF's derivatives are discretized using a centred finite difference method, such that the discretized EEDF is written at the middle of the energy interval.

After the discretization, there is an EBE matrix, and a system can be constructed of which the solution is the EEDF. However, the ionization coefficients are non-linear, as a result an iterative solution must be implemented.

Solving the non-linear EBE

Terms that involve the ionization rate coefficient C_I, or the reduced first Townsend ionization coefficient $\alpha_R = \alpha/N$, are non-linear on the EBE, because the EEDF must be known in order to calculated them.

The ionization rate coefficient can be calculated with,

$$C_I = \sqrt{\frac{2\,e}{m_e}} \int_0^\infty u \sigma_I(u) f(u) du. \tag{30}$$

. The reduced first Townsend ionization coefficient can be calculate using its relation with the net electron production,

$$\alpha_R = \frac{C_I}{v_{drift}}, \tag{31}$$

and with the drift-diffusion equation written on the electron drift velocity

$$v_{drift} = -N\,D\alpha_R + \mu_0 E_{0R}. \tag{32}$$

With these relations, a quadratic equation in α_R can be written, with solution,

$$\alpha_R = \frac{\mu_0 E_{0R} - \sqrt{(\mu_0 E_{0R})^2 - 4NDC_I}}{2ND}. \tag{33}$$

Analytical verification of the discretized electron Boltzmann equation

Analytical verifications of the particle and energy balance identified discretization errors on the ionization collisional operator on the order of the energy step. For the particle balance equation the error was,

$$\mathcal{O}(\Delta u) = \sum_{k=1}^{(n-M_I)2} u_{2k+M_I} q^i_{sec}(u_{2k+M_I}, u_k) f_{2k+M_I} \Delta u^2. \tag{34}$$

For the energy balance equation the error was,

$$\mathcal{O}(\Delta u) = \sum_{k=1}^{(n-M_I)2} u_k u_{2k+M_I} q^i_{sec}(u_{2k+M_I}, u_k) f_{2k+M_I} \Delta u^2. \tag{35}$$

In order to account for these errors the calculation of the C_I coefficient was changed into,

$$C_I = \sqrt{\frac{2\,e}{m_e}} \sum_{k=1}^{n} J_I\Big|_k \Delta u. \tag{36}$$

This procedure ensures a perfect verification of the numerical particle balance equation, and minimizes the relative error of the energy balance equation (keeping it bellow 10^{-12}).

Iterative method

In order to solve the non-linear EBE, the ionization coefficients need to be explicitly calculated, and then iterated until convergence. These coefficients will function as convergence parameters, namely α_R or C_I being the convergence parameter for the spatial or temporal growth model, respectively. The iterative method can be described as follows:

1. An EEDF is calculated without including secondary electrons;
2. Using the previous EEDF as an initial guess, the convergence parameter is calculated;
3. Using the previous value of the convergence parameters, the EBE matrix is constructed now including the production of secondary electrons due to ionization events;
4. The ionization routine cycle commences with a new calculation of the EEDF;
5. The new EEDF is used to update the convergence parameters;
6. The convergence criteria are checked. If convergence is not achieved the cycle continues back to step 3.

Once the convergence criteria are met, usually corresponding to relative differences smaller than 10^{-10} for the convergence parameters and the EEDF, the cycle is terminated. A flow chart of this iterative algorithm can bee seen in Figure 1.

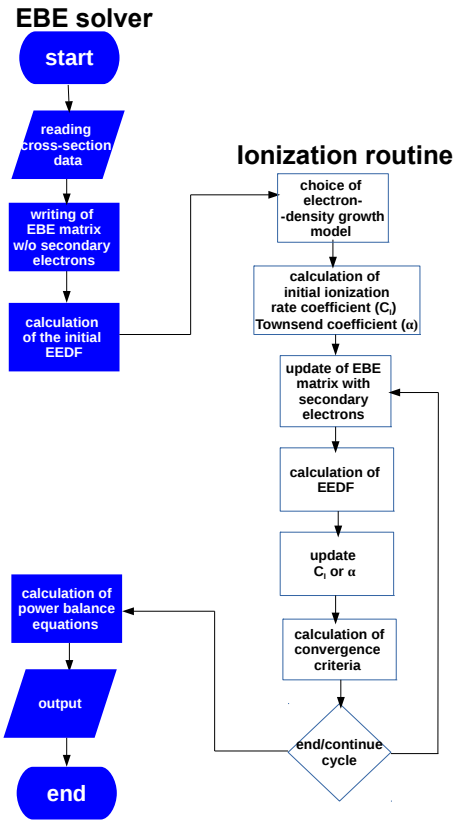

FIG. 1: Flowchart of the EBE solver in LoKI. In blue we present the original routine if secondary electrons were not included. On the right hand side, we present all the various steps of the ionization routine.

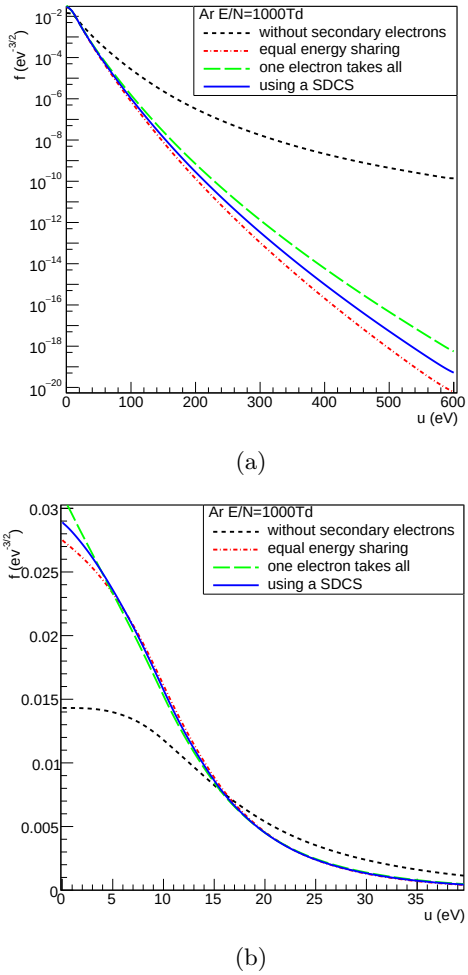

FIG. 2: Plot of EEDFs calculated in LoKI for Argon with DC $E/N = 1000$Td and the electron density spatial growth model.

Coupling with electron-electron collisions

The electron-electron collisional operator (J_{ee}) is non-linear on the EEDF. In LoKI there was a routine in place responsible to iteratively calculate this operator. In order to fully integrate the new treatment of electron-impact ionizations, a coupling between the ionization routine and the electron-electron collisions routine was necessary.

To do this, a global cycle was implemented. This cycle is essentially composed by two steps. On the first step, the ionization routine is performed, in which ionization convergence parameters are iteratively calculated. On the second step, the electron-electron collisions routine is performed, in which the collisional operator is iteratively calculated. The global cycle is then repeated until both the electron-electron collisional operator and the ionization convergence parameter converge.

RESULTS

Comparison between energy sharing models

These tests were performed for Argon, the general behaviour being similar for other gases. A comparison of the three energy sharing models was done for $E/N = 1000$ Td. The different energy sharing effects were similar between growth models, so the comparisons were done for the exponential spatial growth model only (see Figure 2).

Comparison between electron density growth models

The results obtained using these models are shown in Figure 3, for a DC Argon plasma at $E/N = 1000$Td, in which we have also included the case in which secondary electrons are not considered.

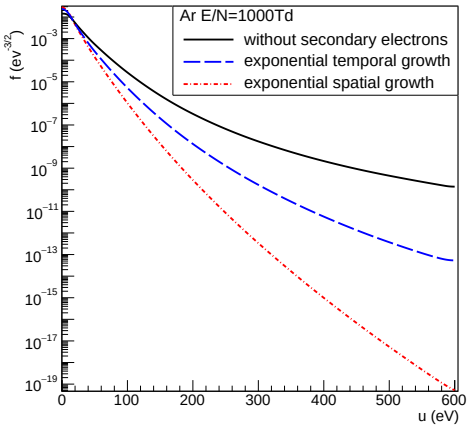

(a)

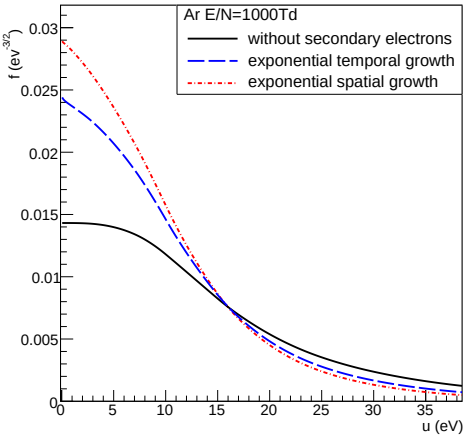

(b)

FIG. 3: Plot of EEDFs calculated in LoKI for Argon with DC $E/N = 1000$Td and the energy sharing using a SDCS.

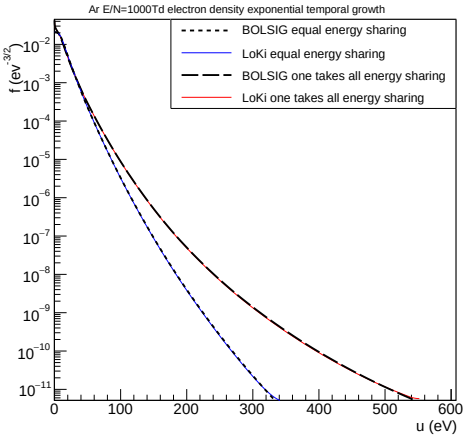

(a) Comparisons between LoKI and BOLSIG+ for different energy sharing in ionization, using the exponential temporal growth model for the electron density.

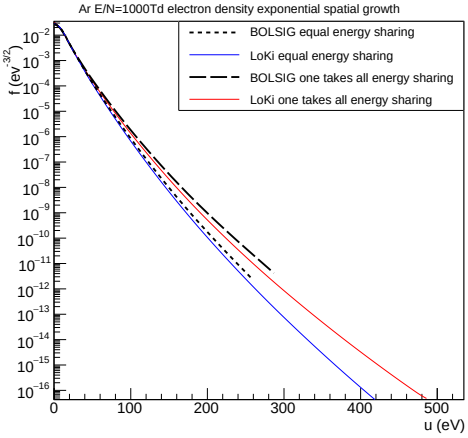

(b) Comparisons between LoKI and BOLSIG+ for different energy sharing in ionization, using the exponential spatial growth model for the electron density

FIG. 4: Comparisons of the EEDF, calculated with LoKI and BOLSIG+, for Argon with DC $E/N = 1000$Td.

Benchmarks against BOLSIG+

The first tests were for the EEDF in Argon at $E/N = 1000$Td, with the temporal growth and the spatial growth models (see Figure 4). After, the first Townsend ionization coefficient, calculated with LoKI and BOLSIG+, was compared for different E/N values in Argon and in molecular Nitrogen (see Figure 5).

Validation of the first Townsend ionization coefficient against experimental data for Ar and N_2

The experiments were made in a Steady State Townsend (SST) discharge, accordingly the spatial electron-density growth model was adopted. Comparisons will use the energy sharing using an SDCS and the case in which secondary electrons are not included.

DISCUSSION

Comparison between energy sharing models

Energy sharing models refers to the way in which the scattered and secondary electrons share the energy available after the ionization collision.

Two limiting cases would be the equal energy sharing, and "one electron takes all" sharing. With equal sharing the secondary electron has always the maximum energy possible and the scattered electron the least energy possible. With the "one electron takes all" the secondary electron has always the minimum possible energy and

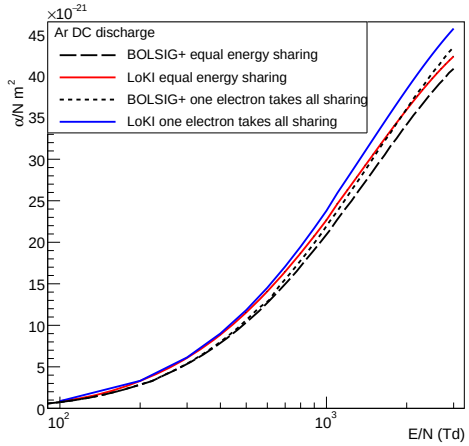

(a) First Townsend ionization coefficient in Argon DC plasmas for various E/N values.

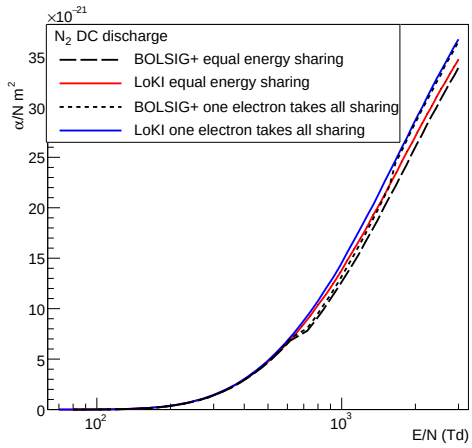

(b) First Townsend ionization coefficient in Nitrogen DC plasmas for various E/N values.

FIG. 5: Comparison between first Townsend ionization coefficient calculated with BOLSIG+ and LoKI.

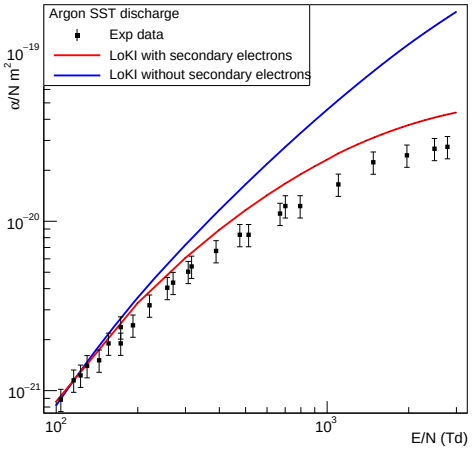

(a) Comparison between LoKI's calculated first Townsend ionization coefficient and experimental data for Argon SST discharges [4].

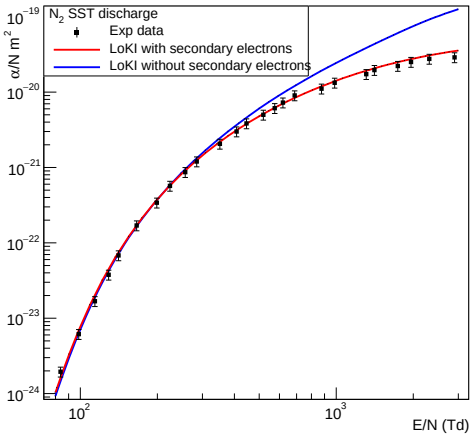

(b) Comparison between LoKI's calculated first Townsend ionization coefficient and experimental data for Nitrogen SST discharges [5].

FIG. 6: First Townsend ionization coefficient as a function of the reduced electric field.

the scattered electron the maximum energy possible. In-between these cases, there is the energy sharing using a SDCS.

Experimental data suggest that there is a maximum near the zero energy of secondary electrons [1, 6], with the lowest probability values being for secondary electrons with energies near its maximum, that is $u_{sec} \approx (\epsilon - V_I)/2$. According to this information, the equal energy sharing scenario would be the least probable one, and the "one electron takes all" the most probable one.

With either spatial or temporal growth, and for both energy sharing modes, there are less high energy electrons when secondary electrons are included. This is caused mostly by the introduction of the secondary electrons at low energies that, by imposing the normalization condition, force the EEDF to be lower at high energy values. This is well illustrated in Figure 2 with the energy sharing mode "one electrons takes all". This mode is in part identical to the treatment of electron-impact ionizations as conservative inelastic collisions, the difference being that here secondary electrons are introduced at zero energy. As a result, the change seems to be caused by the introduction of secondary electrons, and not by the energy partitioning between the electrons produced after the ionization.

In Figure 2a we can better see the behaviour of the high-energy region of the EEDF, mainly correlated with the most energetic of the product electrons, the scattered electron. In the "one takes all" case, the energy of the scattered electrons after the collision has the maximum value $u_{sca} = \epsilon - V_I$. In this case the tail of the EEDF is higher. In contrast, on the equal energy sharing case,

the energy of a scattered electron after the collision is $u_{sca} = (\epsilon - V_I)/2$ which is the lowest possible value for a scattered electron. This shows why this case will have the lowest probability of finding a high energy electron. The tail of the EEDF for the energy sharing using a SDCS is between these two limiting cases.

Observing Figure 2b we can better see the behaviour of the low energy region of the EEDF, mainly related with the energy of the least energetic of the product electrons, the secondary electron. For the "one electron takes all" case, the probability is the highest. This is expected, since with this type of sharing secondary electrons are introduced at zero energy. The EEDF of the equal energy sharing case has the lowest probability (apart from the case without secondary electrons). This can be explained by the fact that with this type of energy sharing, secondary electrons have the highest possible energy $u_{sec} = (\epsilon - V_I)/2$. Again, the case in which the energy sharing is described with a differential ionization cross section is between the limiting cases.

Comparison between electron density growth models

A significant difference is observed between the two growth models. Spatial growth seems to produced lower tails than the temporal growth model, which also relates to a higher probability of finding low energy electrons (see Figure 3).

This result is coherent with lower drift velocities for the spatial growth model, where the electron flux is composed by two opposite components, due to the drift in the electron field and the diffusion caused by a pressure gradient (see relations 24 and 22).

Benchmarks against BOLSIG+

One of the most popular EBE solvers is BOLSIG+ [7]. This EBE solver has some of the electron-density growth models of LoKI. However, it can only use either the equal sharing or the "one electron takes all" energy sharing mode, so our benchmark tests against BOLSIG+ will not include the description of ionization using a SDCS.

Contrary to LoKI, BOLSIG's energy grid is not completely defined by the user [7]. Comparing two distribution functions with different initial and final energy grid points is difficult, since different energy limits can change the EEDF in a significant way when enforcing the normalization condition. So, whenever possible, we have tried to match LoKI's user-defined energy grid with BOLSIG's.

For the exponential temporal growth model there is very good agreement between BOLSIG+ and LoKI for all energy sharing cases (see Figure 4a).

The EEDFs for the exponential spatial growth model are similar in shape, but they don't match as well (see Figure 4b). One of the factors for this discrepancy was the difficulty in matching the energy grid-points. If BOLSIG's upper limit for the energy grid is used in LoKI, large power-balance errors are present. However, even when these limits are made very similar, there are still some differences between the EEDFs that might be due to the distinct discretization procedures in the two EBE solvers.

For the first Townsend ionization coefficient, the EBE solvers predict similar results (see Figure 5). However, there are some deviations for high E/N values in Nitrogen and even for low E/N values in Argon.

Validation of the first Townsend ionization coefficient against experimental data for Ar and N_2

In Argon the simulation predictions improved significantly but they are still above experimental data uncertainty (see Figure 6a). In Nitrogen the inclusion of secondary electrons was enough to shift LoKI's predictions into experimental data uncertainty (see Figure 6b). These results show that LoKI can now operate at higher E/N values.

LoKI does yet not consider attachment or recombination non-conservative process. Since attachment and recombination have an effect on the number of electrons, it may have an influence on the electron density growth terms of the EBE.

In SST experiments, the ejection of electrons from the cathode due to ions or photons is significant. These secondary processes can be difficult to separate from the current growth due to electron impact ionization. Some measurements of the secondary ionization coefficients were made in nitrogen [8], and separated in fast and slow coefficients, due to cathode emissions by ions and by photons or metastables, respectively. With this discrimination of the secondary ionization coefficients, it may be possible to include these processes in the EBE.

The use of the equal energy sharing mode

The non-conservative ionization operator with predefined equal energy sharing is popular in the LTP community, being preferred even when the "one electron takes all" mode is available. This may be because it leads to closer estimates when compared to the experimental data of the first Townsend ionization coefficient (see Figure 7).

Nonetheless, we have seen in this section that the equal energy sharing scenario is much less probable than the "one electron takes all" scenario (when compared to a differential description of the energy sharing), so the better

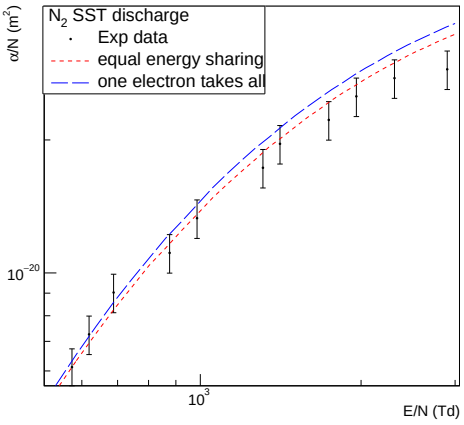

FIG. 7: Comparison between LoKI's calculated first Townsend ionization coefficient with equal energy sharing mode, "one electron takes all" mode, and experimental data for Nitrogen SST discharges [5].

estimates cannot be attributed to a more realistic ionization operator. One of the possibilities, is that the EEDF calculated with the equal energy sharing mode, somehow underestimates the value of the first Townsend ionization coefficient, leading to closer estimates.

However the fact that the equal energy sharing is the least probable scenario means that its use cannot be properly justified with physical arguments.

CONCLUSION

This work as contributed to the LoKI-B code in various ways besides the expected improvements of coefficient predictions for high values of E/N.

The inclusion of an ionization collisional operator allowed for a critical analysis of the most frequently used ionization collisional operators with predefined energy sharing, questioning the use of the equal energy sharing mode.

The inclusion of two electron density growth models will allow users to better tailor their simulations to a specific gas discharge, and it paves the way for the implementation of other non-conservative collisional operators, such as attachment or recombination.

This work also produced important documentation that can support the future development of LoKI-B code.

ACKNOWLEDGEMENTS

I would like to acknowledge the guidance of my supervisor Prof. Luís Lemos Alves. The opportunity to be part of the project KIT-PLASMEBA and liberty to explore the subject further, resulted in a gratifying and interesting work. I thank the team of this project, for even the brief discussions helped me understand and consolidate the study. I genuinely thank Antonio Tejero that was always available to discuss and explain matters whenever I asked.

A special thanks to my family and friends for their support through life.

[1] C. Opal, W. Peterson, and E. Beaty, J. Chem. Phys. **55**, 4100 (1971).
[2] C. Opal, E. Beaty, and W. Peterson, Atomic Data **4**, 209 (1972).
[3] T. Holstein, Phys. Rev. **70**, 367 (1946).
[4] J. V. Božin, Z. M. Jelenak, Z. V. Velikić, I. D. Belča, Z. L. Petrović, and B. M. Jelenković, Phys. Rev. E **53**, 4007 (1996).
[5] M. A. Folkard and S. C. Haydon, Journal of Physics B: Atomic and Molecular Physics **6**, 214 (1973).
[6] J. T. Grissom, R. N. Compton, and W. R. Garrett, Phys. Rev. A **6**, 977 (1972).
[7] G. J. M. Hagelaar and L. C. Pitchford, Plasma Sources Sci. Technol. **14**, 722 (2005).
[8] S. C. Haydon and O. M. Williams, Journal of Physics D: Applied Physics **9**, 523 (1976).